JACS
JOURNAL OF THE AMERICAN CHEMICAL SOCIETY
pubs.acs.org/JACS
Article

A Shapeshifting Roadmap for Polycyclic Skeletal Evolution

Andre Sanchez, Anjali Gurajapu, Wentao Guo,[§] Wang-Yeuk Kong,[§] Croix J. Laconsay,[§] Nicholas S. Settineri, Dean J. Tantillo,* and Thomas J. Maimone*

Cite This: J. Am. Chem. Soc. 2023, 145, 13452−13461
Read Online
ACCESS | Metrics & More | Article Recommendations | Supporting Information

ABSTRACT: Polycyclic ring systems are ubiquitous three-dimensional (3D) structural motifs central to the function of many biologically active small molecules and organic materials. Indeed, subtle changes to the overall molecular shape and connectivity of atoms in a polycyclic framework (i.e., isomerism) can drastically alter its function and properties. Unfortunately, direct evaluation of these structure−function relationships typically requires the development of distinct synthetic strategies toward a specific isomer. Dynamic, "shapeshifting" carbon cages present a promising approach for sampling isomeric chemical space but are often difficult to control and are largely limited to thermodynamic mixtures of positional isomers about a single core scaffold. Here, we describe the development of a new shapeshifting C9-chemotype and a chemical blueprint for its evolution into structurally and energetically diverse isomeric ring systems. By leveraging the unique molecular topology of π-orbitals interacting through-space (homoconjugation), a common skeletal ancestor evolved into a complex network of valence isomers. This unusual system represents an exceedingly rare small molecule capable of undergoing controllable and continuous isomerization processes through the iterative use of just two chemical steps (light and organic base). Computational and photophysical studies of the isomer network provide fundamental insight into the reactivity, mechanism, and role of homoconjugative interactions. Importantly, these insights may inform the rational design and synthesis of new dynamic, shapeshifting systems. We anticipate this process could be a powerful tool for the synthesis of structurally diverse, isomeric polycycles central to many bioactive small molecules and functional organic materials.

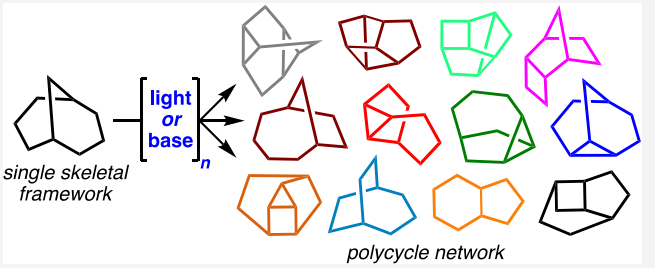

INTRODUCTION

The three-dimensional (3D) shape and arrangement of functional groups within an organic small molecule govern its interactions with biological targets.[1] Polycyclic ring systems have emerged as powerful tools for controlling the arrangement of atoms in 3D space. These rigid structural motifs are used extensively by organisms evolving beneficial secondary metabolites[2,3] (alkaloids, polyketides, and terpenes) as well as medicinal chemists pursuing new small-molecule therapeutics.[4−7] Polycyclic $C_9(sp^3)$-rich scaffolds are a particularly privileged structural motif found in thousands of natural products with biological relevance to human disease, but present significant synthetic challenges in the laboratory.[8−10] Indeed, the development of strategies for the efficient construction of congested carbocyclic frameworks is often a central focus and bottleneck in natural product synthesis programs.[8,11,12] In this context, deceptively simple changes in the connectivity of polycyclic ring systems (i.e., stereochemical and constitutional isomerism) can often require the redesign of synthetic strategies entirely.[5,8] This adds considerably to the cost and complexity of synthesis, particularly in programs that value the exploration of diverse chemical space.[13,14] To this end, the development of a unified approach for the interconversion and preparation of polycyclic scaffolds from a more synthetically accessible isomer could be enabling for the synthesis of natural[15−17] and unnatural[18,19] products for drug discovery and materials[20] applications.

Isomerization reactions present one strategy to modify the shape of a molecule without changing its atomic composition. Moreover, isomerism (stereochemical, positional, or skeletal) can profoundly alter the biological activity and physiochemical properties of drug leads[21] and natural metabolites[16,17] (Figure 1A). For example, the cytotoxic natural products clusianone (**2**) and nemorosone (**3**), which are positional isomers around an otherwise conserved bicyclo[3.3.1]nonane core, promote protonophoric mitochondrial uncoupling, yet do so with altered efficacy.[16] Similarly, the alkaloid cyclopamine (**4**) promotes the cyclopia phenotype in developing zebrafish embryos, while its skeletal isomer cyclopamine A (**5**) is functionally inactive.[17] While methods for the selective late-stage isomerization[22−24] of small molecules have become increasingly important in this regard, synthetic processes that enable both the positional and skeletal isomerism of

Received: April 17, 2023
Published: June 6, 2023

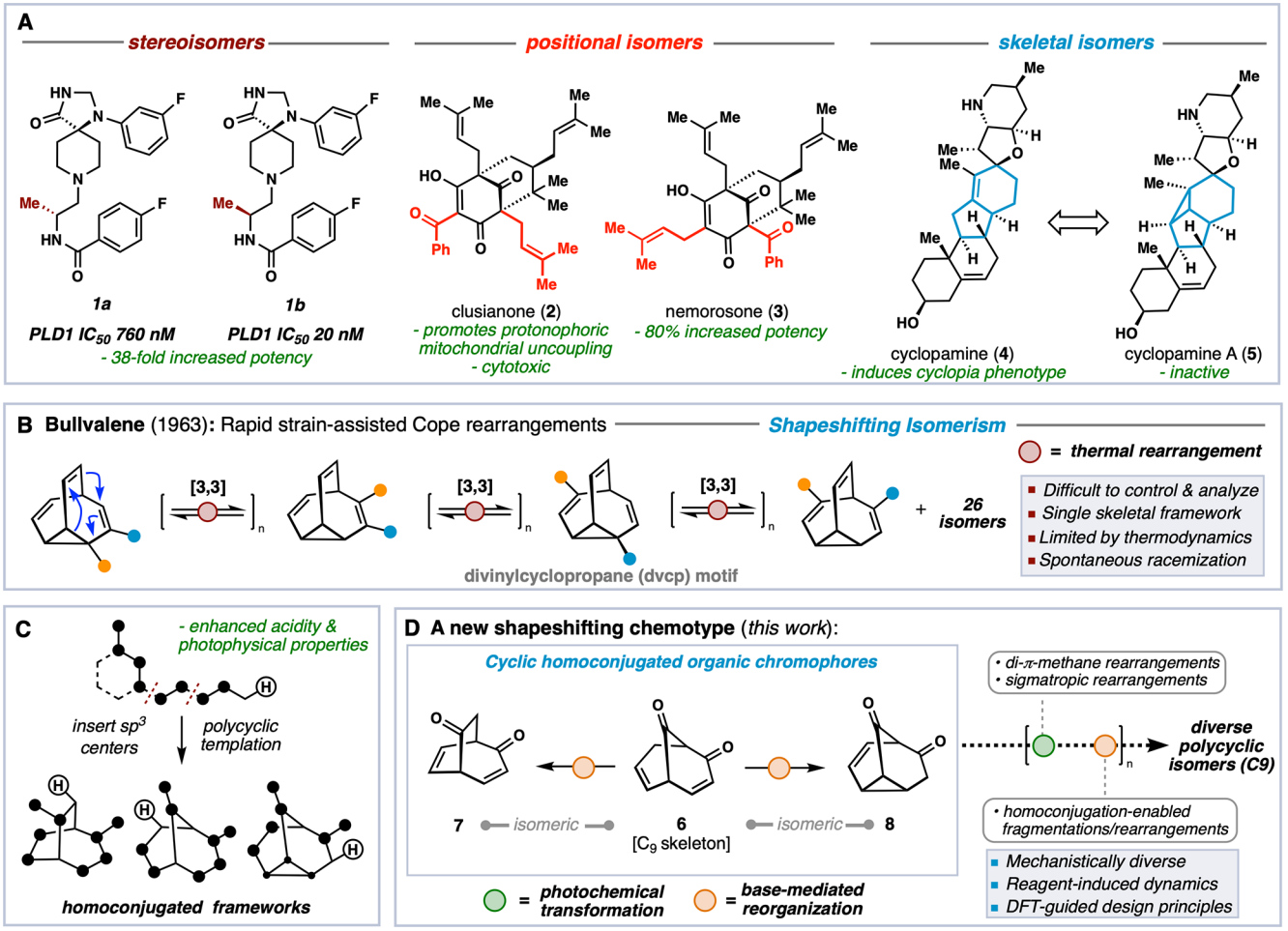

Figure 1. Molecular shape isomerism. (A) Functional impact of positional, skeletal, and stereoisomerism in organic small molecules. (B) Canonical strategies for shapeshifting isomerism in polycyclic frameworks. (C) Topological representation of spatially interacting orbitals in rigid, homoconjugated C9-scaffolds. (D) Proposed process for skeletal evolution wherein iterative rounds of homoconjugation-enabled anionic and photochemical rearrangements continuously transform a readily accessible bicycle into a family of diverse polycyclic isomers.

carbocyclic frameworks remain rare and underexplored.[25] Such reactions pose a significant challenge because they often require inert covalent bonds (carbon-carbon) to be selectively broken and reformed—effectively shuffling the connectivity of core atoms in a molecule.

Constitutionally dynamic (shapeshifting) carbon frameworks, which undergo rapid and continuous valence reorganization through thermal pericyclic rearrangements, present an intriguing solution for exploring isomeric chemical space (Figure 1B).[26] Since Doering and Roth's seminal proposal in 1963, neutral, shapeshifting carbon cages such as bullvalene have predominantly featured strain-assisted Cope rearrangements as the molecular mechanism imparting fluxionality.[26−28] While powerful, these thermal isomerizations produce dynamic, equilibrium mixtures of interconverting positional isomers about a single carbon skeleton, presenting a fundamental limitation to the molecular shapes accessible.[26] Moreover, these rapidly interconverting small molecules are inherently challenging to control, capture, and analyze, making subsequent structure−function relationships difficult to ascertain and presenting a daunting challenge to their translation in a synthetic setting.[29−31]

Motivated by the challenges and prospects of utilizing shapeshifting molecules, we sought to develop a complementary, but mechanistically distinct approach for the synthesis of structurally and energetically diverse polycyclic isomers. We envisioned that a chemical blueprint for the mild valence restructuring of polycyclic frameworks could be potentially enabling for discovery programs through the late-stage, spatial reorientation of groups central to the function of organic small molecules. In formalizing such a strategy, we recognized the need to identify a unique shapeshifting chemotype and distinct triggering event(s) to explore a new dynamic, reactivity space.

RESULTS AND DISCUSSION

Development of a Skeletal Evolution Strategy. Conjugation is a phenomenon frequently exploited in organic synthesis and materials chemistry.[32,33] Indeed, planar (or nearly so) topologies of directly interacting π-systems often impart enhanced stability and useful photophysical properties in chemical systems.[33] However, the chemical consequences of homoconjugation—the orbital overlap of weakly interacting π-systems separated by a nonconjugating group—have been far less appreciated and studied, especially in the context of synthesis.[34−37] Our group recently leveraged this concept to enable remote allylic functionalization in the total synthesis of the polyketide natural product, ocellatusone C.[38] In that work, we discovered a base-mediated isomerization reaction relating discrete skeletal isomers through a dynamic, shapeshifting

https://doi.org/10.1021/jacs.3c03960
J. Am. Chem. Soc. 2023, 145, 13452−13461

Scheme 1. Light Initiated Evolution of C9 Topological Diversity[a]

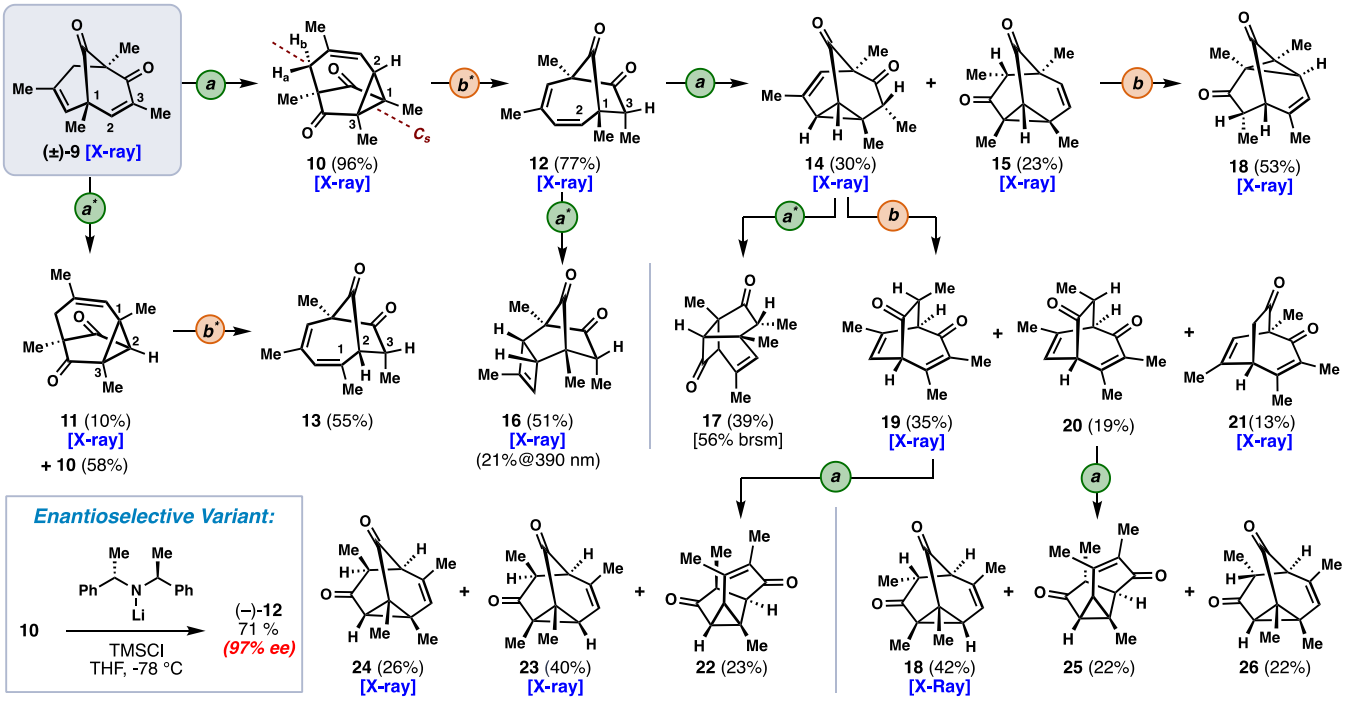

[a]Iterative rounds of photomediated and anionic rearrangements yield precise and mild atomic reorganization to a diverse reaction network of positional, skeletal, and stereoisomers. **Reaction conditions:** (*a*) 390 nm violet LED, MeCN; (*a**) 300 nm UV, MeCN, quartz tube; (*b*) KHMDS, PhMe/THF, −78 °C; (*b**) KHMDS, PhMe/THF, 0 °C.

anion. We thought this unusual shapeshifting C9-chemotype could serve as a promising entry point for exploring skeletal dynamics but would likely be limited to a thermodynamic mixture of isomers. We recognized that this entire skeletal network (**6**−**8**), however, possessed mixed chromophores embedded in rigid, homoconjugated frameworks, defined by interacting π- and Walsh-type cyclopropane orbitals in spatially precise configurations[39−41] (Figure 1C,D). We reasoned that the subtle spatial differences between these interacting orbitals (whether they engage in homoconjugation in energy minima or along reaction coordinates) would lead to distinct, but conserved reactivity profiles among isomers. Therefore, we anticipated that photochemical isomerization[42−44] of these systems would result in a network of diverse photoisomers not constrained by thermodynamics. We hypothesized that the resulting valence isomers, retaining interacting π-systems or strained rings with enhanced *p*-character,[39−41] could then be subjected to thermal, base-induced[31,38] reorganizations to regenerate mixed chromophores. By the continuous coupling of photochemical[42−44] and base-induced[31,38] shapeshifting rearrangements, we anticipated we would be able to structurally "evolve" a single skeletal framework into a network of its positional, skeletal, and stereoisomers (Figure 1D).

Here, we report the development of this shapeshifting paradigm, highlighting the synthetic potential of the underutilized concept of homoconjugation.[34] Guided by computational and experimental insights, recursive cycles of photo- and base-mediated reactions continuously transform a common skeletal framework into structurally and energetically diverse polycycles. We further demonstrate the power of this strategy in a highly enantioselective valence restructuring, providing an enantioenriched skeletal feedstock for inclusion into this process. Finally, we show that a single modification to the periphery of these polycyclic systems can lead to divergent skeletal evolution, providing an additional variable that can be adjusted to yield distinct ring topologies.

Light Initiated Skeletal Evolution. Our studies toward the development of a shapeshifting strategy for polycyclic skeletal evolution commenced with the homoconjugated bicyclo[3.3.1]nonane-containing enone **9** (Scheme 1).[38] This tetrasubstituted model C9-chemotype, which can be prepared in gram quantities in six steps with minimal purifications,[38] served to simplify characterization and mechanistic analyses of the expected complex network of isomers. We envisioned that upon photoirradiation, **9** would either undergo di-π-methane (DPM) or oxa-di-π-methane (ODPM) rearrangements to yield a tricyclo[4.2.1.$0^{2,8}$]nonane nucleus (see the "Plausible mechanism" appendix in the Supporting Information for more details). In principle, both reaction paths are possible given the presence of mixed 1,4-diene and ß,γ-unsaturated ketone chromophores.[42,43] Although DPM-type rearrangements often require triplet sensitization, this and many other reactions of this unique homoconjugated chemotype proceeded directly at relatively long wavelengths without the need for external photocatalysts.[42,45,46] Accordingly, direct photoirradiation using a 390 nm violet LED lamp provided C_s-symmetric tricyclo[4.2.1.$0^{2,8}$]nonane **10** in 96% yield as a single skeletal isomer, presumably through a wavelength-selective DPM rearrangement. Interestingly, using higher-energy (300 nm) UV-B irradiation also afforded **10** (58% yield), in addition to its positional isomer **11** in 10% yield, likely through an ODPM rearrangement. These results are consistent with the UV−visible absorption profile of this network of photoisomers (**9**−**11**) and a presumed photostationary state, highlighting the subtle, but chemically mean-

https://doi.org/10.1021/jacs.3c03960
J. Am. Chem. Soc. 2023, 145, 13452−13461

Scheme 2. Base-Initiated Evolution of C9 Topological Diversity[a]

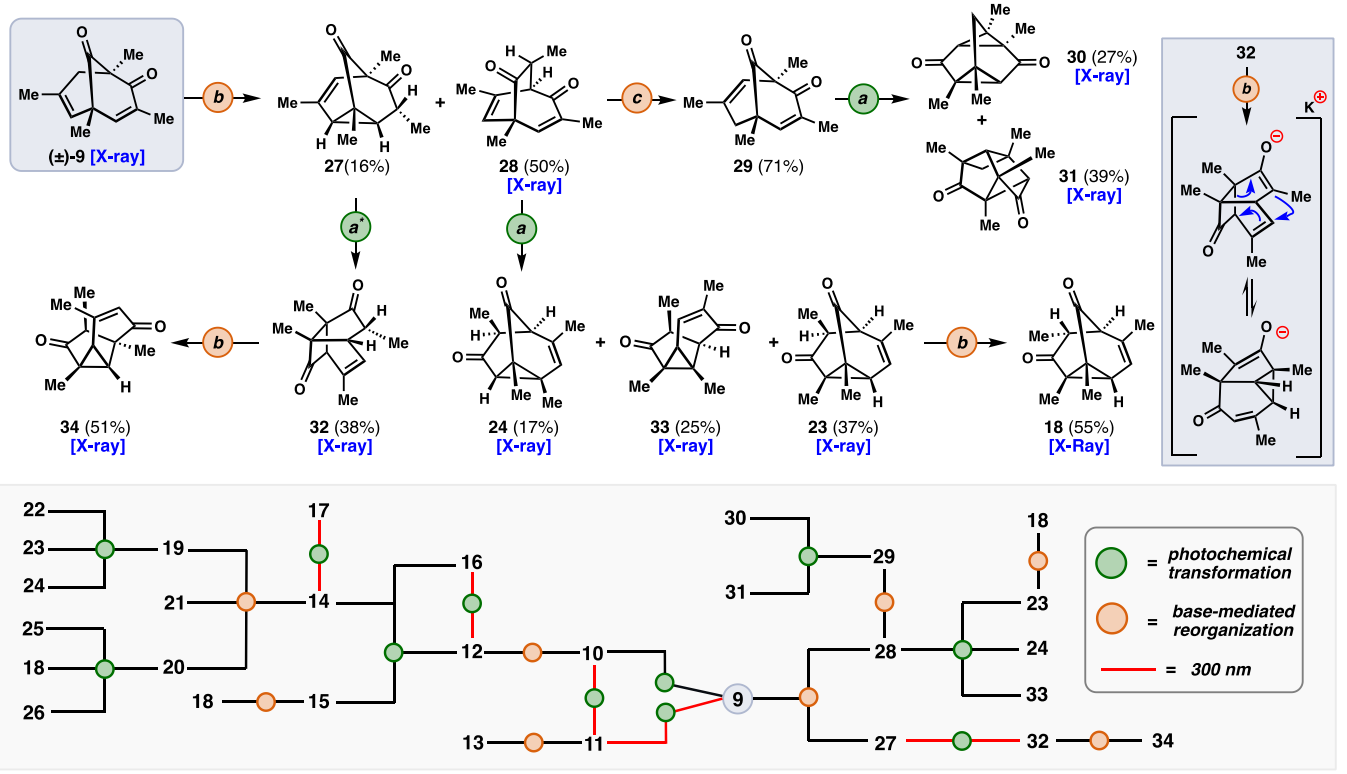

[a]The ordering of synthetic operations can further diversify the polycycle library as represented graphically by the depicted valence isomer network. **Reaction conditions:** (*a*) 390 nm violet LED, MeCN; (*a**) 300 nm UV, MeCN, quartz tube; (*b*) KHMDS, PhMe/THF, −78 °C; (*c*) KO*t*Bu, EtOH, −10 °C

ingful photophysical differences among isomers (see "UV−vis spectra" appendix in the Supporting Information).

Inspired by the enhanced acidity of homoconjugated frameworks,[47,48] we hypothesized that remote allylic deprotonation of the tricyclo[4.2.1.$0^{2,8}$]nonane nucleus may lead to further valence restructuring through strain-promoted cyclopropane fragmentation. As expected, base-induced fragmentation of **10**, followed by aqueous quenching, afforded bicyclo[4.2.1]nonane-containing ketone **12** as a single diastereo- and skeletal isomer in 77% yield. Isomer **11** also selectively afforded the corresponding skeletal isomer **13** in 55% yield under these reaction conditions. Remarkably, this reaction could be rendered highly enantioselective (97% e.e.) by employing a commercially derived chiral lithium amide base to desymmetrize compound **10** (see inset, Scheme 1). Importantly, the base-mediated restructuring of **10** regenerated mixed ODPM-type chromophores (ß,γ-unsaturated carbonyls) for further cycling in this strategy. Direct photoirradiation of **12** (at 390 nm) afforded a mixture of tricyclo[3.3.1.$0^{2,8}$]-nonane-containing skeletal isomers **14** and **15** along with cyclobutene-containing **16** in 74% combined isolated yield (~2:1:1 ratio in crude photolysis mixture). Recognizing the presence of an additional ODPM chromophore, we reasoned it may be possible to further evolve isomer **14** photochemically. Guided by its UV−visible absorption profile, sequential photoirradiation of **14** at 300 nm produced tricyclo[4.3.0.$0^{3,9}$]-nonane **17**, likely through a vinylogous-ODPM-type rearrangement. On the other hand, irradiating **12** directly at 300 nm provided cyclobutene **16** as the major skeletal isomer. These results illustrate the ability to rationally select distinct isomers by exploiting subtle differences in the photophysical properties of mixed chromophores and the wavelength of light used.[42,43]

Following these photorearrangements, we sought to investigate the base-driven evolution of the rigid tricyclo-[3.3.1.$0^{2,8}$]nonane core. Structurally, positional isomers **14** and **15** differ in the placement of a carbonyl group within their core framework. We reasoned that this subtle difference in structure (and π-orbital placement) would result in distinct shapeshifting isomerization pathways. Accordingly, treatment of **15** with KHMDS at −78 °C afforded the positional isomer **18** in 53% yield, likely from a rapid Cope rearrangement of a barbaralone-enolate intermediate (see "Mechanistic studies and free energy profiles" in the Supporting Information). Subjecting **14** to the same reaction conditions, however, provided a mixture of bicyclo[3.2.2]nonane positional isomers (**19**−**21**) with regenerated DPM-type chromophores for further photochemical cycling. Gratifyingly, direct photoirradiation of bicyclo[3.2.2]-nonane **19** at 390 nm proceeded readily to afford tricyclo-[3.3.1.$0^{2,8}$]nonanes **23** and **24**, as well as the skeletal isomer **22** in 89% combined yield. Irradiation of the diastereomeric bicyclo[3.2.2]nonane **20** proceeded similarly, producing isomers **18**, **25**, and **26**, and highlighting the ability of this strategy to rapidly sample skeletal, positional, and stereochemical space.

Base Initiated Skeletal Evolution. We next turned our attention to the ordering of synthetic operations. In principle, our recursive skeletal evolution strategy could be initiated by either light- or base-mediated rearrangements. We reasoned that these reactions would result in distinct structural isomers by exploiting differences in homoconjugation. Following our initial work, base-promoted isomerization of bicyclo[3.3.1]-

https://doi.org/10.1021/jacs.3c03960
J. Am. Chem. Soc. 2023, 145, 13452−13461

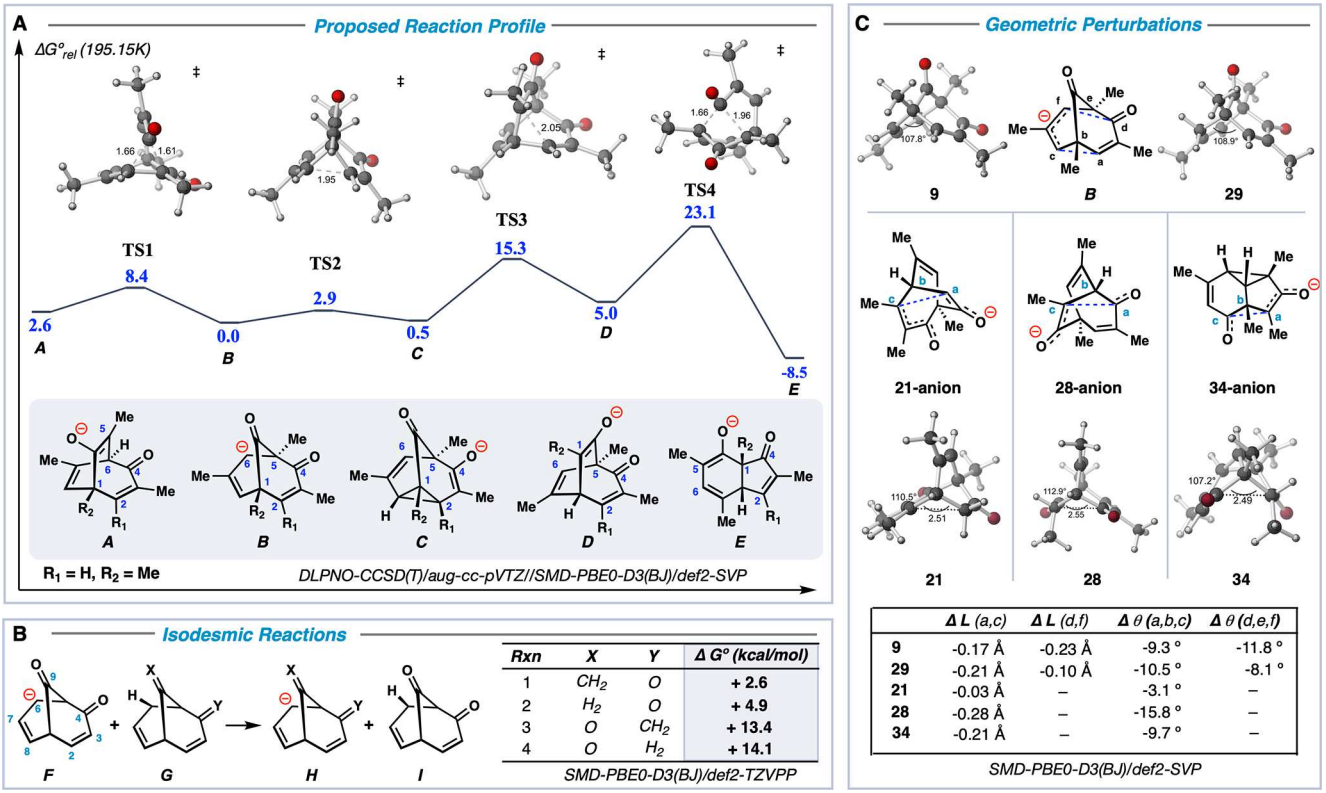

Figure 2. DFT and *ab initio* studies on shapeshifting anions. (A) Calculated free energy profile relating isomeric anions. (B) Isodesmic reactions to probe structural features important for anion stability. (C) Structural evidence for homoconjugative stabilization in polycyclic anions.

nonane **9** provided tricyclo[3.3.1.0^{2,8}]nonane-containing ketone **27** and bicyclo[3.2.2]nonane-containing enone **28** as a mixture of skeletal isomers, while maintaining mixed chromophores (Scheme 2).[38] Subsequent photoirradiation of **27** at 300 nm resulted in selective valence restructuring to the tricyclo[4.3.0.0^{3,9}]nonane **32** in 38% yield. Notably, this tricyclic skeletal isomer, which is distinct from previously prepared **17**, possesses a strained cyclobutanone moiety, which we hypothesized could participate in an anion-induced fragmentation.[41] Accordingly, treatment of **32** with KHMDS at −78 °C provided skeletal isomer **34** in 51% yield, presumably through an unusual divinylcyclopropyl ⇋ divinylcyclobutyl enolate equilibrium (see inset, Scheme 2). On the other hand, direct photoirradiation of enone **28** at 390 nm afforded tricyclo[3.3.1.0^{2,8}]nonanes **23** and **24**, as well as the skeletal isomer **33** in 79% combined yield. Expectedly, subjecting **23** to base, followed by quenching with aqueous solution, resulted in selective epimerization to diastereomer **18**.

Inspired by the adaptive nature of dynamic, shapeshifting equilibria,[26,29−31] we wondered if we could chemically direct our anionic rearrangements by interrupting the suspected ion-pairing with potassium cations.[38] Guided by our calculations,[38] we hypothesized that cation solvation could bias the anionic equilibrium, driving the reaction to the more stable bicyclo[3.3.1]nonane skeleton. Indeed, treatment of bicyclo[3.2.2]nonane **28** with KO*t*Bu in EtOH at −10 °C resulted in thermodynamic isomerization to bicyclo[3.3.1]-nonane **29** in 71% yield. We were cognizant that the formal positional isomerism of **9** to **29** would likely have photochemical consequences, and indeed, direct photoirradiation of **29** using a 390 nm violet LED lamp provided a mixture of triasteranedione **30** and strained quadricycle **31** in 66% combined yield.

Interestingly, this double ODPM-type synthesis of triasteranediones resembles early work by Mellor et al. from a related isomeric bicyclo[3.3.1]nonane core.[49] These preliminary studies establish the feasibility of this shapeshifting strategy to access a complex network of diverse polycyclic isomers originating from a common skeletal ancestor (see bottom of Scheme 2). Analyzing the network of skeletal isomers related to **9** reveals that a comprehensive set of polycyclic frameworks can be accessed by a sequence of only five facile chemical transformations.

Computational Insights on Shapeshifting Anions. To better understand the base-mediated rearrangements that enable skeletal evolution and the potential role of homoconjugation, we first investigated the shapeshifting mechanism originating from carbanion **B** (Figure 2A). Isomeric anions and transition structures (TSs) along the plausible reaction pathway were studied with density functional theory (DFT) calculations. We employed the SMD(THF)-PBE0-D3(BJ)/def2-SVP level of theory to optimize isomers and transition structures. Relative free energies were computed from higher-level single points at DLPNO-CCSD(T)/aug-cc-pVTZ and Gibbs free energy corrections at 195.15 K from the level used for optimization (see the "Computational details" in the Supporting Information for more details). Contrary to our initial proposal involving a stepwise Cope/cyclopropoxide-anion fragmentation mechanism,[38] calculations revealed that anion **B** can convert directly to bicyclo[3.2.2]nonane-containing carbanion **A** through a reversible [1,2]-sigmatropic rearrangement via **TS1** with a barrier of only 8.4 kcal·mol^{-1}. Alternatively, **B** can isomerize to the barbaralone-enolate **C** via

https://doi.org/10.1021/jacs.3c03960
J. Am. Chem. Soc. 2023, 145, 13452−13461

Scheme 3. Substituent Effects[a]

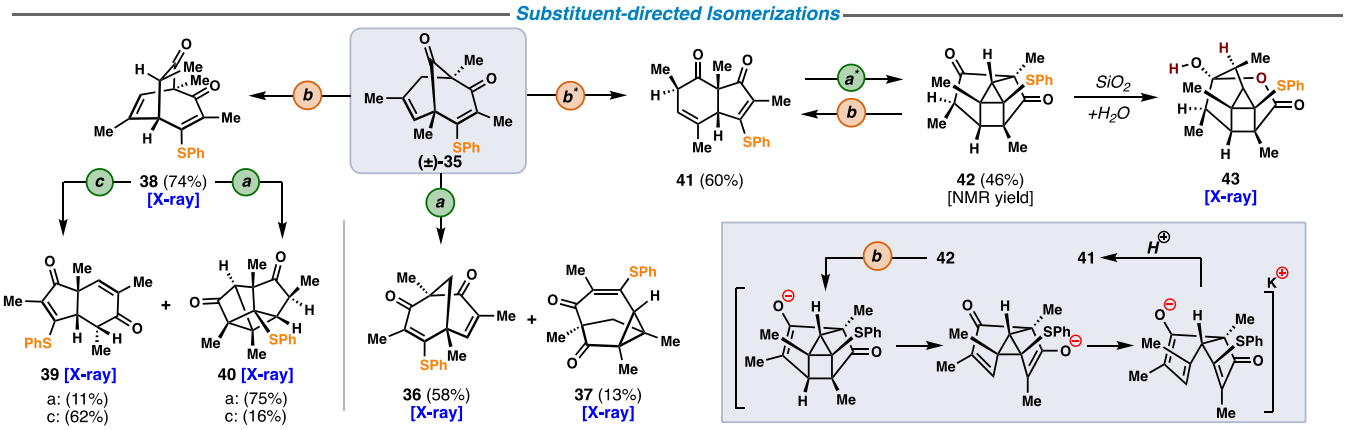

[a]A heteroatom substituent allows for distinct photochemical and anionic rearrangements enabling access to new skeletons. **Reaction conditions:** (*a*) 390 nm violet LED, MeCN; (*a**) 350 nm UV, MeCN, quartz tube; (*b*) KHMDS, PhMe/THF, −78 °C; (*b**) KHMDS, PhMe/THF, 0 °C; (*c*) 390 nm violet LED, CyH.

TS2 with a remarkably low barrier of 2.9 kcal·mol^{-1}. The isomeric bicyclo[3.2.2]nonane-containing carbanion **D** can then originate from a retro-Michael-type fragmentation via **TS3**. Notably, these calculations led to the unexpected discovery of a [1,3]-sigmatropic shift relating **D** to bicyclo[4.3.0]nonane-containing carbanion **E** via **TS4**, albeit with a relatively high predicted overall barrier of 23 kcal·mol^{-1} (at 195.15 K). Extending these calculations to an isomeric scaffold derived from tricyclo[3.3.1.0^{2,8}]nonane **14** (R_1 = Me, R_2 = H) had little impact on the reaction profile (see "Mechanistic studies and free energy profiles" in the Supporting Information).

The two sigmatropic rearrangements (via **TS1** and **TS4**) are of note, since both involve ostensibly suprafacial/suprafacial migrations involving four electrons and should therefore be forbidden by the Woodward−Hoffmann orbital symmetry rules under the thermal conditions used.[50] Nonetheless, both have rather low barriers. To reveal the origins of these low barriers, we carried out detailed investigations of the intrinsic reaction coordinates (IRCs) for each reaction (see "Computational details" in the Supporting Information for more details). Being concerted does not guarantee synchronous bond-making and bond-breaking, which provides one avenue for avoiding penalties associated with orbital symmetry forbiddenness.[51−53] However, Mayer bond order (MBO) analysis indicated that the bond-breaking and bond-forming events occur synchronously for both reactions.[54] In both steps, the carbonyl π-bond (C4 = O) is first weakened and then slowly recovers, indicating that participation of the adjacent π_{C-O}* orbital facilitates these anionic migrations.[55,56] Population analysis using the CHELPG (CHarges from ELectrostatic Potentials using a Grid-based method) scheme also indicates negative charge accumulation and release about the carbonyl oxygen during both reactions. Thus, these rearrangements circumvent the Woodward−Hoffmann rules by exploiting the interaction of orthogonal orbitals at the migrating carbon, thereby enabling a pseudopericyclic or coarctate reaction.[57,58] Importantly, the compact structure of the polycyclic hydrocarbons studied here, which position multiple π-systems in proximity (homoconjugation), appears to facilitate these processes. These calculations further expand the mechanistic set of known reactions amenable to rapid shapeshifting dynamics.[26]

To gain deeper insight into the structural and electronic features of the proximal, potentially homoconjugated, π-systems, we probed through-space charge delocalization using a variety of computed isodesmic reactions (e.g., Figure 2B).[59] These suggest that the degree of homoconjugation present in **B** is significant. For instance, all else being equal, altering the bridge carbonyl oxygen in the simplified carbanion **F** to CH_2—and balancing the rest of the isodesmic reaction—resulted in a 2.6 kcal·mol^{-1} free energy difference, which suggests that carbanion **F** is slightly stabilized by the carbonyl oxygen (*Rxn 1*). However, the same analysis resulted in differences of 4.9 and 13.4 kcal·mol^{-1} for removing the bridge C9-carbonyl altogether and altering the C4-carbonyl to CH_2, respectively (*Rxn 2 and 3*). These results are consistent with a considerable degree of homoconjugation.[47] Geometry changes also support this view: the interbridge angle of $\angle C_a$-C_b-C_c in anion **B** contracts from 109° in the neutral structure **29**, and from 108° in neutral structure **9**, to 99° in the anionic structure (Figure 2C). Similar geometric changes in other isomeric polycyclic anions indicate the presence of general homoconjugative interactions across a wide range of structures, albeit to varying degrees. These results reinforce the notion that spatially preorganized carbocyclic frameworks can facilitate the stabilization of reactive intermediates and further expand the scope of known valence isomerization reactions.

Substituent-Directed Shape Divergence. We next investigated the impact of electronically modulating our homoconjugated frameworks with an electron-donating substituent. We reasoned that slight electronic perturbation of our rigid π-network may enable distinct photo- and base-mediated rearrangements. We commenced our studies with the bathochromically shifted vinylogous thioester **35** (Scheme 3).[38] Direct photoirradiation of **35** at 390 nm resulted in a divergent photochemical [1,3]-sigmatropic rearrangement, affording bicyclo[3.3.1]nonane **36** in 58% yield. Notably, **35** and **36** differ only in the placement of a single carbonyl oxygen atom. Tricyclo[4.2.1.0^{2,8}]nonane-containing isomer **37** was also formed in 13% yield, presumably through a DPM rearrangement. Unfortunately, attempts to further evolve **36** through base-mediated rearrangement were unsuccessful, resulting in complex, intractable reaction mixtures. By changing the ordering of synthetic operations, however, **35**

https://doi.org/10.1021/jacs.3c03960
J. Am. Chem. Soc. 2023, 145, 13452−13461

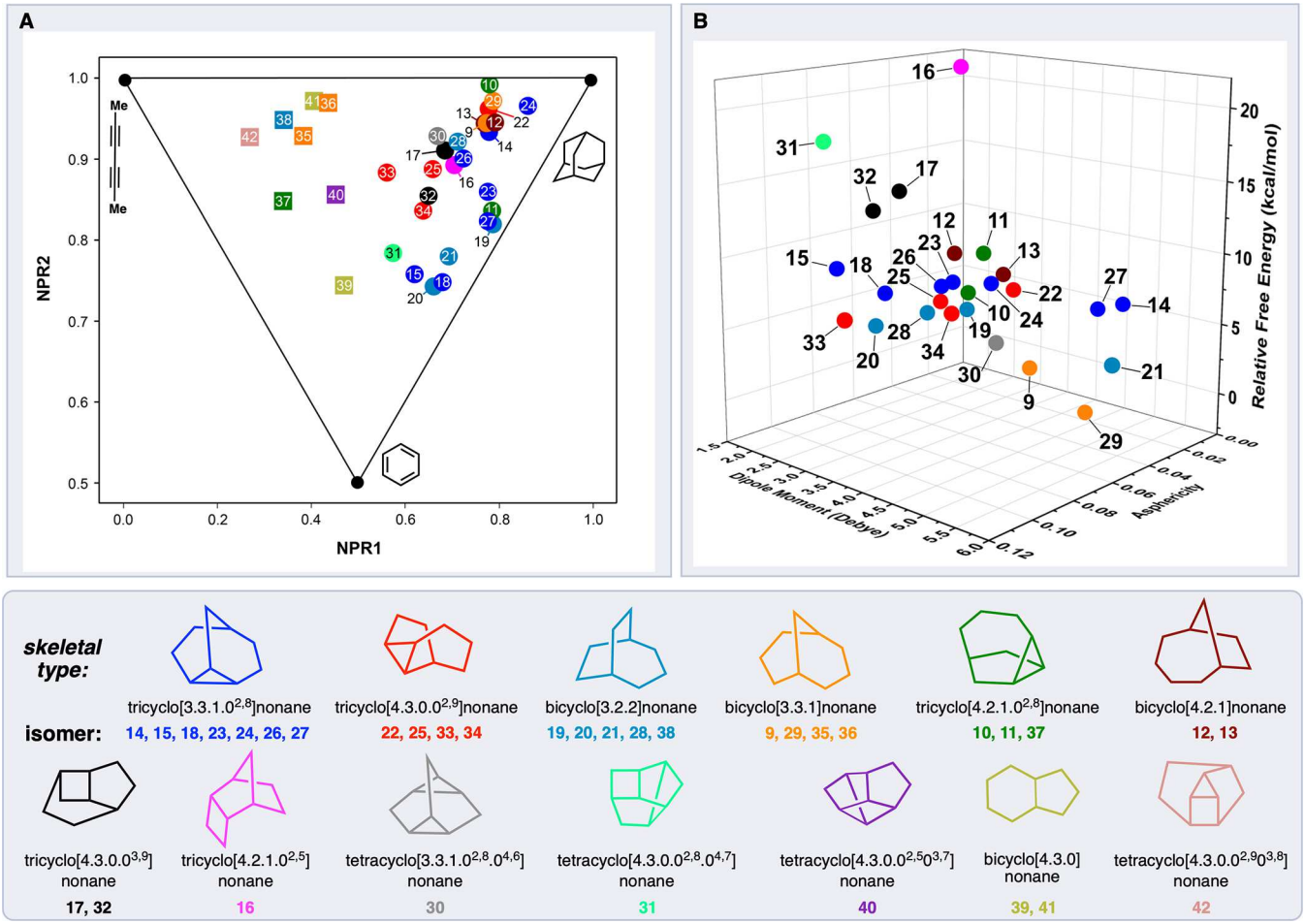

Figure 3. Chemoinformatic analysis of polycycle network. (A) Shape analysis using a triangular PMI plot derived from a synthesized library of skeletal frameworks derived from **9** (circle markers) and **35** (square markers). Typical molecules representing linear, spherical, and "pancake" shapes are shown near the appropriate corners of the plot. (B) Visualization of three-dimensional shape, electronic, and energetic diversity of developed valence network derived from bicycle **9**.

selectively evolved to skeletal isomer **38** in 74% yield.[38] Subsequent photoirradiation, and [1,3]-sigmatropic rearrangement, in cyclohexane then afforded bicyclo[4.3.0]nonane **39** in 62% yield as a major isomer. In this case, we found that this reaction was sensitive to the solvent used, unexpectedly evolving **38** to quadricycle **40** (75% yield) when MeCN was employed (see "Plausible mechanism" appendix in the Supporting Information for more details). To better understand the impact of substituents on the shapeshifting dynamics, we computed the reaction profile for the carbanion derived from **35**. Interestingly, we noted the hypothetical process involving a [1,3]-sigmatropic rearrangement had a considerably lower overall activation barrier ($\Delta G^{\ddagger}$ = 19.0 kcal·mol^{-1}) compared to the previously computed rearrangement to form **E** ($\Delta G^{\ddagger}$ = 23.1 kcal·mol^{-1}). We hypothesized that this step may be surmountable at higher temperatures. Gratifyingly, treatment of bicyclo[3.3.1]nonane **35** with KHMDS at −78 °C, followed by gentle warming to 0 °C, led to the selective formation of bicyclo[4.3.0]nonane-containing isomer **41** in 60% yield. Again, this base-induced rearrangement process regenerated chromophores for further skeletal evolution. Guided by its UV−visible absorption profile, direct photoirradiation of **41** at 350 nm afforded the hindered cycloadduct **42**, which was partially converted to **43** during purification on silica gel. As before, we anticipated that base-mediated fragmentation of the cyclobutane ring system would regenerate reactive chromophores. Indeed, treatment of the strained housane **42** with KHMDS returned the bicyclo[4.3.0]nonane nucleus, presumably via the depicted fragmentations (see inset, Scheme 3). Importantly, all of the base-induced, thermal rearrangements presented here could be reliably predicted (and/or rationalized) through quantum chemical calculations (see "Mechanistic studies and free energy profiles" in the Supporting Information).

Chemoinformatic Insights. Having developed a mechanistically distinct shapeshifting chemotype, and a conceptual framework for its skeletal evolution, we sought to apply chemoinformatic techniques to better understand the structural and energetic diversity of the polycyclic library formed. Visualization of the normalized principal moments of inertia (NPR)[60] for our compound library indicated that most isomers possess a significant degree of spherical character, as evidenced by their clustering toward the right edge of the principal moments of inertia (PMI) plot (Figure 3A). Interestingly, our plot also suggests that this three-dimensionality (expressed as NPR[60]) is quite sensitive to positional and stereochemical isomerism (Figure 3A) in addition to skeletal isomerism. For example, the tricyclo[3.3.1.0^{2,8}]nonane-containing isomers (colored in dark blue), which only differ in the placement of substituents about a conserved core, are evenly

https://doi.org/10.1021/jacs.3c03960
J. Am. Chem. Soc. 2023, 145, 13452−13461

distributed along the upper half of the disk-sphere edge in the PMI plot. The structures prepared here could potentially serve as diverse templates for sampling 3D chemical space—a property that is increasingly important in drug discovery.[13,14]

This plot further illustrates the power of this skeletal evolution approach to explore diverse, isomeric 3D shapes originating from a single bicyclo[3.3.1]nonane ancestor (**9**) (colored in orange). We next plotted the dipole moment, molecular asphericity,[61] and relative free energies of the library of isomers evolved from **9** (Figure 3B). As shown in Figure 3B, these valence isomers display diverse ranges of dipole moment (spanning over 3.5 Debye)—a feature that may be useful for reorienting polar vectors or pharmacophores in drug development[4−7] (see Figure S52 for a 2D projection of dipole moment and energy). Finally, free energy analysis of this network (relative to **9**) suggests that the skeletal framework contributes most significantly to the energy differences among isomers. The wide range of free energies (exceeding 24 kcal·mol^{-1}) captured overall demonstrates the ability to continuously traverse the energy surface of polycyclic C9-isomers via the coupling of base- and light-mediated rearrangement processes. This contrasts with purely thermodynamically controlled isomerization strategies in synthesis, especially those based solely on thermal pericyclic reactions.

CONCLUSIONS

In summary, nearly 35 distinct isomeric polycycles, spanning 13 ring systems, were accessed from a single bicyclo[3.3.1]-nonane skeleton through the iterative application of just two mild chemical steps. Through detailed computational studies, we delineated fundamental principles to rationalize and guide the development of this skeletal evolution strategy. Our findings also uncovered that the base-mediated rearrangements in this system are mechanistically distinct from the canonical Cope- or β-scission/cyclization-type rearrangements common to bullvalene and related shapeshifting molecules. Through chemoinformatic analyses, we established that this process can greatly expand the diversity of 3D molecular shapes, dipole moments, and energetics. Importantly, this work lays the foundation for a next-generation, tractable shapeshifting chemotype with the potential to access underexplored molecular shapes. We envision this process could be a powerful tool for evaluating isomeric, but structurally diverse, polycycles central to many bioactive small molecules[15−19] and organic materials.[20]

ASSOCIATED CONTENT

Data Availability Statement

All reported data can be found in the manuscript and the Supporting Information. Requests for additional materials should be directed to the corresponding authors. X-ray crystallographic data for **9−12, 14−16, 18, 19, 21, 23, 24, 28, 30−34, 36−40, 43, and SI-6** are available from the Cambridge Crystallographic Data Centre under CCDC #'s 2238125, 2238124, 2238123, 2254805, 2238135, 2238130, 2238138, 2238140, 2238133, 2238129, 2238134, 2238141, 2157567, 2238126, 2238137, 228128, 2238132, 2238139, 2238142, 2238131, 2157566, 2238143, 2238136, 2238144, and 2238127. Computational data and relevant files are available at the ioChem-BD repository *via* https://iochem-bd.bsc.es/browse/handle/100/275146;

Supporting Information

The Supporting Information is available free of charge at https://pubs.acs.org/doi/10.1021/jacs.3c03960.

Experimental, computational, and spectroscopic data (PDF)

Accession Codes

CCDC 2238123−2238144 and 2254805 contain the supplementary crystallographic data for this paper. These data can be obtained free of charge via www.ccdc.cam.ac.uk/data_request/cif, or by emailing data_request@ccdc.cam.ac.uk, or by contacting The Cambridge Crystallographic Data Centre, 12 Union Road, Cambridge CB2 1EZ, UK; fax: +44 1223 336033.

AUTHOR INFORMATION

Corresponding Authors

Dean J. Tantillo − *Department of Chemistry, University of California−Davis, Davis, California 95616, United States;* orcid.org/0000-0002-2992-8844; Email: djtantillo@ucdavis.edu

Thomas J. Maimone − *Department of Chemistry, University of California−Berkeley, Berkeley, California 94720, United States;* orcid.org/0000-0001-5823-692X; Email: maimone@berkeley.edu

Authors

Andre Sanchez − *Department of Chemistry, University of California−Berkeley, Berkeley, California 94720, United States;* orcid.org/0000-0001-7047-5077

Anjali Gurajapu − *Department of Chemistry, University of California−Berkeley, Berkeley, California 94720, United States*

Wentao Guo − *Department of Chemistry, University of California−Davis, Davis, California 95616, United States*

Wang-Yeuk Kong − *Department of Chemistry, University of California−Davis, Davis, California 95616, United States;* orcid.org/0000-0002-4592-0666

Croix J. Laconsay − *Department of Chemistry, University of California−Davis, Davis, California 95616, United States;* orcid.org/0000-0002-9244-1318

Nicholas S. Settineri − *Department of Chemistry, University of California−Berkeley, Berkeley, California 94720, United States;* orcid.org/0000-0003-0272-454X

Complete contact information is available at: https://pubs.acs.org/10.1021/jacs.3c03960

Author Contributions

[§]W.G., W.-Y.K., and C.J.L. contributed equally to this work.

Funding

This work was supported by the National Institutes of Health (grant S10OD024998 funding the 600-MHz cryoprobe, grant S10-RR027172 for X-ray crystallographic resources, and grant S10OD023532 funding the Molecular Graphics and Computation Facility at UC Berkeley); the National Science Foundation (Predoctoral Fellowship DGE-1752814 and DGE-2146752 to A.S.); the Ford Foundation (Predoctoral Fellowship to A.S.); UC Berkeley (Chancellor's Graduate Fellowship to A.S.); the American Chemical Society Division of Organic Chemistry (ACS DOC-SURF Fellowship to A.G.); and the National Science Foundation (CHE-2154083 and the XSEDE program via CHE030089 supporting the computational work at UC Davis).

Notes

The authors declare no competing financial interest.

■ ACKNOWLEDGMENTS

The authors thank Dr. Hasan Celik and UC Berkeley's NMR facility in the College of Chemistry (CoC NMR) for spectroscopic assistance. They are grateful to Dr. Cooper Citek and Alex Wheeler (UC Berkeley) for assistance with UV−vis measurements. They also thank Dr. Ulla Andersen and Dr. Zhongrui Zhou for mass spectrometry analysis.

■ REFERENCES

(1) Leach, A. R.; Gillet, V. J.; Lewis, R. A.; Taylor, R. Three-Dimensional Pharmacophore Methods in Drug Discovery. *J. Med. Chem.* **2010**, *53*, 539−558.
(2) Bornancin, L.; Bonnard, I.; Mills, S. C.; Banaigs, B. Chemical mediation as a structuring element in marine gastropod predator-prey interactions. *Nat. Prod. Rep.* **2017**, *34*, 644−676.
(3) Le Bideau, F.; Kousara, M.; Chen, L.; Wei, L.; Dumas, F. Tricyclic Sesquiterpenes from Marine Origin. *Chem. Rev.* **2017**, *117*, 6110−6159.
(4) Taylor, R. D.; MacCoss, M.; Lawson, A. D. G. Rings in Drugs. *J. Med. Chem.* **2014**, *57*, 5845−5859.
(5) Subbaiah, M. A. M.; Meanwell, N. A. Bioisosteres of the Phenyl Ring: Recent Strategic Applications in Lead Optimization and Drug Design. *J. Med. Chem.* **2021**, *64*, 14046−14128.
(6) Auberson, Y. P.; Brocklehurst, C.; Furegati, M.; Fessard, T. C.; Koch, G.; Decker, A.; La Vecchia, L.; Briard, E. Improving Nonspecific Binding and Solubility: Bicycloalkyl Groups and Cubanes as *para*-Phenyl Bioisosteres. *Chem. Med. Chem.* **2017**, *12*, 590−598.
(7) Stockdale, T. P.; Williams, C. M. Pharmaceuticals that contain polycyclic hydrocarbon scaffolds. *Chem. Soc. Rev.* **2015**, *44*, 7737−7763.
(8) Yang, X. W.; Grossman, R. B.; Xu, G. Research Progress of Polycyclic Polyprenylated Acylphloroglucinols. *Chem. Soc. Rev.* **2018**, *118*, 3508.
(9) Shi, Z.; Hu, H.; Guo, Y.; Duan, Y.; Zhang, Y.; et al. Discovery of 13,15-*nor*polycylic polyprenylated acylphloroglucinols from *Hypericum longistylum* with anti-inflammatory activity. *Org. Biomol. Chem.* **2022**, *20*, 1284.
(10) Jeker, O. F.; Carreira, E. M. Total Synthesis and Stereochemical Reassignment of (±)-Indoxamycin B. *Angew. Chem., Int. Ed.* **2012**, *51*, 3464−3477.
(11) Ting, C. P.; Maimone, T. J. Total Synthesis of Hyperforin. *J. Am. Chem. Soc.* **2015**, *137*, 10516.
(12) Shen, X.; Ting, C. P.; Xu, G.; Maimone, T. J. Programmable Meroterpene Synthesis. *Nat. Commun.* **2020**, *11*, No. 508.
(13) Lovering, F.; Bikker, J.; Humblet, C. Escape from Flatland: Increasing Saturation as an Approach to Improving Clinical Success. *J. Med. Chem.* **2009**, *52*, 6752−6756.
(14) Lovering, F. Escape from Flatland 2: complexity and promiscuity. *Med. Chem. Comm.* **2013**, *4*, 515−519.
(15) Shen, L.; Zou, X. P.; Li, W. S.; Mándi, A.; Kurtán, T.; Wu, J. Granatripodins A−B, limonoids featuring a Tricyclo[3.3.1.$0^{2,8}$]nonane motif: Absolute configuration and agnostic effects on human pregnane−X−receptor. *Bio. Chem.* **2021**, *111*, No. 10488.
(16) Reis, F. H. Z.; Pardo-Andreu, G. L.; Nuñez-Figueredo, Y.; Cuesta-Rubio, O.; Marín-Prida, J.; Uyemura, S. A.; Curti, C.; Alberici, L. C. Clusianone, a naturally occurring nemorosone regioisomer, uncouples rat liver mitochondria and induces HepG2 cell death. *Chem.-Biol. Interact.* **2014**, *212*, 20−29.
(17) Liu, Q. X.; Yuan, X.; Ye, J.; Yue, R. C.; Shen, Y. H.; Shan, L.; Li, H. L.; Zhang, W. D. Isolation, identification, and bioactivity of microbial metabolites of cyclopamine and its congeners. *Phytochem. Lett.* **2015**, *12*, 203−208.
(18) Motoyama, K.; Nagata, T.; Kobayashi, J.; Nakamura, A.; Miyoshi, N.; Kazui, M.; Sakurai, K.; Sakakura, T. Discovery of a bicyclo[4.3.0]nonane derivative DS88790512 as a potent, selective, and orally bioavailable blocker of transient receptor potential canonical 6 (TRPC6). *Bioorg. Med. Chem. Lett.* **2018**, *28*, 2222−2227.
(19) Karageorgis, G.; Foley, D. J.; Laraia, L.; Brakmann, S.; Waldmann, H. Pseudo Natural Products− Chemical Evolution of Natural Product Structure. *Angew. Chem., Int. Ed.* **2021**, *60*, 15705−15723.
(20) Warrener, R. N.; Abbenante, G.; Solomon, R. G.; Russell, R. A. Homoladderanes: A Chevron-shaped Motif for Molecular Design. *Tetrahedron Lett.* **1994**, *35*, 7639−7642.
(21) O'Reilly, M. C.; Scott, S. A.; Brown, K. A.; Oguin, T. H.; Thomas, P. G.; Daniels, J. S.; Morrison, R.; Brown, H. A.; Lindsley, C. W. Development of Dual PLD1/2 and PLD2 Selective Inhibitors from a Common 1,3,8-Triazaspiro[4.5]decane Core: Discovery of ML298 and ML299 That Decrease Invasive Migration in U87-MG Glioblastoma Cells. *J. Med. Chem.* **2013**, *56*, 2695−2699.
(22) Wang, P. Z.; Xiao, W. J.; Chen, J. R. Light-empowered contra-thermodynamic stereochemical editing. *Nat. Rev. Chem.* **2023**, *7*, 35−50.
(23) Wang, Y.; Hu, X.; Morales-Rivera, C. A.; Li, G.-X.; Huang, X.; He, G.; Liu, P.; Chen, G. Epimerization of Tertiary Carbon Centers via Reversible Radical Cleavage of Unactivated C(sp^3)−H Bonds. *J. Am. Chem. Soc.* **2018**, *140*, 9678−9684.
(24) Zhang, Y. A.; Palani, V.; Seim, A. E.; Wang, Y.; Wang, K. J.; Wendlandt, A. E. Stereochemical editing logic powered by the epimerization of unactivated tertiary stereocenters. *Science* **2022**, *378*, 383−389.
(25) Scott, L. T.; Jones, M. Rearrangements and Interconversions of Compounds of Formula (CH)n. *Chem. Rev.* **1972**, *72*, 181.
(26) (a) Bismillah, A. N.; Chapin, B. M.; Hussein, B. A.; McGonigal, P. R. Shapeshifting molecules: the story so far and the shape of things to come. *Chem. Sci.* **2020**, *11*, 324−332. (b) Karton, A. Shapeshifting radicals. *Chem. Phys.* **2022**, *552*, No. 111373.
(27) Doering, W. von E.; Roth, W. R. A Rapidly Reversible Degenerate Cope Rearrangement. *Tetrahedron* **1963**, *19*, 715−737.
(28) Doering, W. von E.; Ferrier, B. M.; Fossel, E. T.; Hartenstein, J. H.; Jones, M.; Klumpp, G.; Rubin, R. M.; Saunders, M. A. A rational synthesis of bullvalene barbaralone and derivatives; bullvalone. *Tetrahedron* **1967**, *23*, 3943−3963.
(29) He, M.; Bode, J. W. Racemization as a stereochemical measure of dynamics and robustness in shape-shifting organic molecules. *Proc. Natl. Acad. Sci. U.S.A.* **2011**, *108*, 14752−14756.
(30) Lippert, A. R.; Naganawa, A.; Keleshian, V. L.; Bode, J. W. Synthesis of Phototrappable Shape-shifting Molecules for Adaptive Guest Binding. *J. Am. Chem. Soc.* **2010**, *132*, 15790−15799.
(31) Lippert, A. R.; Kaeobarmrung, J.; Bode, J. W. Synthesis of Oligosubstituted Bullvalones: Shapeshifting Molecules Under Basic Conditions. *J. Am. Chem. Soc.* **2006**, *128*, 14738−14739.
(32) Wang, Y.; Liu, H.; Paan, Q.; Wu, C.; Hao, W.; Xu, J.; Chen, R.; Liu, J.; Li, Z.; Zhao, Y. Construction of Fully Conjugated Covalent Organic Frameworks via Facile Linkage Conversion for Efficient Photoenzymatic Catalysis. *J. Am. Chem. Soc.* **2020**, *142*, 5958−5963.
(33) Thomas, S. W.; Joly, G. D.; Swager, T. M. Chemical Sensors Based on Amplifying Fluorescent Conjugated Polymers. *Chem. Rev.* **2007**, *107*, 1339−1386.
(34) Scott, L. T. Cyclic Homoconjugation in Neutral Organic-Molecules. *Pure Appl. Chem.* **1986**, *58*, 105−110.
(35) Doerner, T.; Gleiter, R.; Robbins, T. A.; Chayangkoon, P.; Lightner, D. A. Homoconjugation and Transannular Orbital Interactions Detected by Photoelectron and carbon-13 NMR Spectroscopy. Bicyclo[3.3.1]Nona-3,7-Diene-2,6-Dione and Bicyclo[3.3.1]-Nonane-2,6-Dione. *J. Am. Chem. Soc.* **1992**, *114*, 3235.
(36) Paquette, L. A.; Wingard, R. E.; Meisinger, R. H. Bishomoconjugative Alpha-Halo Ketone Rearrangement as a Route to Bicyclo[4.2.1]Nona-2,4,7-Trien-9-One and Barbaralone Derivatives. *J. Am. Chem. Soc.* **1972**, *94*, 2155.
(37) Tran Ngoc, T.; Grabicki, N.; Irran, E.; Dumele, O.; Teichert, J. F. Photoswitching neutral homoaromatic hydrocarbons. *Nat. Chem.* **2023**, *15*, 377−385.

https://doi.org/10.1021/jacs.3c03960
J. Am. Chem. Soc. 2023, 145, 13452−13461

(38) Sanchez, A.; Maimone, T. J. Taming Shapeshifting Anions: Total Synthesis of Ocellatusone C. *J. Am. Chem. Soc.* **2022**, *144*, 7594−7599.
(39) Goldstein, M. J.; Hoffmann, R. Symmetry, Topology, and Aromaticity. *J. Am. Chem. Soc.* **1971**, *93*, 6193.
(40) Childs, R. F.; Cremer, D.; Elia, G. Cyclopropyl Homoconjugation−Experimental Facts and Interpretations. In *The Chemistry of the Cyclopropyl Group*; Patai, S.; Rappoport, Z.; Rappoport, Z., Eds.; John Wiley & Sons, Ltd., 1995; pp 411−468.
(41) Gleiter, R.; Schafer, W. Interactions between Nonconjugated π-Systems. *Acc. Chem. Res.* **1990**, *23*, 369−375.
(42) Zimmerman, H. E.; Armesto, D. Synthetic aspects of the di-π-methane rearrangement. *Chem. Rev.* **1996**, *96*, 3065−3112.
(43) Houk, K. N. Photochemistry and Spectroscopy of β,γ-Unsaturated Carbonyl-Compounds. *Chem. Rev.* **1976**, *76*, 1−74.
(44) Kärkäs, M. D.; Porco, J. A.; Stephenson, C. R. J. Photochemical Approaches to Complex Chemotypes: Applications in Natural Product Synthesis. *Chem. Rev.* **2016**, *116*, 9683−9747.
(45) Maiti, B. C.; Lahiri, S. S. Photoreactivity in δ-keto-β,γ-enones: oxa-di-π-methane (ODPM) rearrangements from states other than T_1 (π, π*). *J. Photochem. Photobiol., A* **1995**, *91*, 27−32.
(46) Goodell, J. R.; Poole, J. L.; Beeler, A. B.; Aube, J.; Porco, J. A. Synthesis and Reactivity of Bicyclo[3.2.1]octanoid-Derived Cyclopropanes. *J. Org. Chem.* **2011**, *76*, 9792−9800.
(47) Brown, J. M. Origins of Stabilization and Evidence for Charge Delocalization in the Bicyclo[3.2.1]octadienyl Anion and Related Species. *Aust. J. Chem.* **2014**, *67*, 1296−1300.
(48) Moncur, M. V.; Grutzner, J. B. Bicyclo[3.2.2]Nona-2,6-Dienyl Carbanion- Preparation, Basicity, and Laticyclic Stabilization. *J. Am. Chem. Soc.* **1973**, *95*, 6449.
(49) Knott, P. A.; Mellor, J. M. Photochemical Rearrangement of Bicyclo[3,3,1]Nona-3,7-Diene-2,6-Diones. *J. Chem. Soc., Perkin Trans. 1* **1972**, *8*, 1030.
(50) Woodward, R. B.; Hoffmann, R. The conservation of orbital symmetry. *Angew. Chem., Int. Ed.* **1969**, *8*, 781−853.
(51) Beno, B. R.; Houk, K. N.; Singleton, D. A. Synchronous or asynchronous? An "experimental" transition state from a direct comparison of experimental and theoretical kinetic isotope effects for a Diels− Alder reaction. *J. Am. Chem. Soc.* **1996**, *118*, 9984−9985.
(52) Singleton, D. A.; Schulmeier, B. E.; Hang, C.; Thomas, A. A.; Leung, S. W.; Merrigan, S. R. Isotope effects and the distinction between synchronous, asynchronous, and stepwise Diels−Alder reactions. *Tetrahedron* **2001**, *57*, 5149−5160.
(53) Tantillo, D. J. Recent excursions to the borderlands between the realms of concerted and stepwise: carbocation cascades in natural products biosynthesis. *J. Phys. Org. Chem.* **2008**, *21*, 561−570.
(54) Mayer, I. Bond order and valence indices: A personal account. *J. Comput. Chem.* **2007**, *28*, 204−221.
(55) Semmelhack, M. F.; Weller, H. N.; Foos, J. S. Thermal rearrangements of spiro [4.4] nonapolyenes. Unusually rapid 1, 5-vinyl migration. *J. Am. Chem. Soc.* **1977**, *99*, 292−294.
(56) Le Drian, C.; Vogel, P. Acid-Catalyzed Rearrangements of 5,6-exo-Epoxy-7-oxabicyclo[2.2.1]hept-2-yl Derivatives. Migratory Aptitudes of Acyl vs. Alkyl Groups in Wagner-Meerwein Transpositions. *Helv. Chim. Acta* **1987**, *70*, 1703−1720.
(57) Herges, R. Coarctate and pseudocoarctate reactions: Stereochemical rules. *J. Org. Chem.* **2015**, *80*, 11869−11876.
(58) Birney, D. M. Theory, experiment and unusual features of potential energy surfaces of pericyclic and pseudopericyclic reactions with sequential transition structures. *Curr. Org. Chem.* **2010**, *14*, 1658−1668.
(59) Wheeler, S. E.; Houk, K. N.; Schleyer, P. V. R.; Allen, W. D. Hierarchy of Homodesmotic Reactions for Thermochemistry. *J. Am. Chem. Soc.* **2009**, *131*, 2547−2560.
(60) Sauer, W. H. B.; Schwarz, M. K. Molecular Shape Diversity of Combinatorial Libraries: A Prerequisite for Broad Bioactivity. *J. Chem. Inf. Comput. Sci.* **2003**, *43*, 987−1003.
(61) Arteca, G. A. Molecular Shape Descriptors. In *Reviews in Computational Chemistry*; Lipkowitz, K. B.; Boyd, D. B., Eds.; John Wiley & Sons, Ltd., 1996.

https://doi.org/10.1021/jacs.3c03960
J. Am. Chem. Soc. 2023, 145, 13452−13461